European Review for Medical and Pharmacological Sciences 2024; 28: 899-906

Magnetic resonance imaging assessment of substantia nigral iron deposition in Parkinson's disease: a meta-analysis

G.-L. LIU[1], H.-W. ZHANG[2], C.-B. ZHA[1], T.-W. FAN[1], S.-T. CHEN[1], T.-T. SHEN[1], K. HE[3]

[1]Department of Neurology, Shanghai Electric Power Hospital, Shanghai, China
[2]Department of Neurology, Laixi People's Hospital, Laixi, Shangdong, China
[3]Ward of No. 1 High Dependency Unit, Changshu Mingzhou Rehabilitation Hospital, Changshu, Jiangsu, China

Abstract. – OBJECTIVE: The pathogenesis of Parkinson's disease (PD) is associated with abnormal iron accumulation. Magnetic resonance imaging (MRI) studies have shown that patients with Parkinson's disease have an increased amount of iron in their substantia nigra (SN). We have undertaken a meta-analysis of studies using MRI in PD, to explore the potential role of MRI in diagnosing PD using abnormal iron deposition in SN as a candidate biomarker.

MATERIALS AND METHODS: Searches of PubMed, Embase, and Medline databases revealed 16 studies that compared PD patients and healthy controls (HC). A sensitivity analysis and subgroup analysis were performed to evaluate the reliability of our results. Estimates were pooled by the fixed-effects model. As an expression of I^2, we computed the proportion of variation due to heterogeneity.

RESULTS: We included 16 studies with sample sizes of 435 PD and 355 HC in our meta-analysis. Results showed that SN iron deposition was significantly elevated ($p<0.00001$) in patients with PD compared to HC ones (SMD=0.72, 95% confidence interval 0.57 to 0.87, $p<0.00001$).

CONCLUSIONS: Our findings, based on a homogeneous group-level analysis, suggest that MRI-based SN iron deposition could be used to distinguish PD from HC. For a more rigorous investigation of SN iron deposition in PD, larger cohort studies are needed.

Key Words:
Magnetic resonance, Imaging assessment, Substantia nigral iron deposition, Parkinson's disease, Meta-analysis.

Introduction

Globally, Parkinson's disease is the second most common neurodegenerative disorder[1]. In Parkinson's disease (PD), dopaminergic neurons in the substantia nigra (SN) are lost[2]. The main diagnostic criteria for Parkinson's disease remain bradykinesia plus rigidity accompanied by resting tremor, which often occur years after the onset of the disease[1]. Although the diagnostic criteria have been revised, delayed diagnosis or misdiagnosis of PD often occurs because there are many clinical similarities in parkinsonism[3]. In order to make an early diagnosis of PD before motor symptoms appear, numerous efforts have been made to explore biomarkers of PD[4]. At present, biomarkers mainly focus on symptom evaluation, specific neuroimaging changes, and biochemical determination of biological fluids in PD. Some biomarkers are being tested in clinical trials to provide value for the diagnosis and prognosis of PD[5].

In 1924, Lhermitte et al[6] demonstrated abnormal iron deposition in PD brain autopsies. Over the course of the next 90 years, this abnormal iron accumulation has been linked to the pathogenesis of PD; with the elevated iron levels within the SN of patients with PD being linked to dopaminergic neuronal cell death[7]. Labile iron in parkinsonian SN generated higher reactive oxygen species activity, thus leads to the death of dopaminergic neurons in SN[8]. Iron is paramagnetic in the living brain tissue, whose evaluation could be obtained from various magnetic resonance (MR) imaging[9]. This has led to the assumption that evaluation of brain iron deposition *via* MR imaging might be used to diagnose and monitor the progression of PD.

T2 or T2*-based method, which can capture the presence of paramagnetic ions such as tissue iron, has been applied to assess the iron of SN in PD patients. Additional proton spin dephasing induces microscopic magnetic fields surrounding the iron deposits, leading to a loss of signals and

Corresponding Author: Kai He, MD; e-mail: hekai@evacoco.cn

causing a strong shortening of T2 or T2* relaxation time. T2 or T2* relaxation rate (1/T2=R2, 1/T2*=R2*) then increases by iron concentration in PD patients[10]. Wallis et al[11] demonstrated that calculated R2' (R2'= R2*- R2) *via* partially refocused interleaved multiple echo (PRIME) MRI sequence can also quantify brain iron in PD patients. Using a PRIME MRI sequence, R2' may be calculated since both R2 and R2* information can be achieved from a single scan[11]. Susceptibility-Weighted Imaging (SWI) is a novel useful three-dimensional gradient echo sequence. Signals from susceptible substances difference between tissues generate various contrast from high-pass filtered SWI phase images[12]. Relative to its surrounding tissues, changes in the amount of iron will result in changes in the phase of the tissue, thus it can be used to quantify iron concentration of tissues. Using this methodology, increased iron deposition could be detected by MRI in the SN of patients in PD patients[9,13].

In this study, we aimed to undertake a meta-analysis of MRI-based studies comparing the iron deposition in SN in idiopathic PD patients and healthy controls (HC) and explore the potential role of MRI in the diagnosis of PD.

Materials and Methods

Search Strategies and Study Selection

The literature encompassed in this research comprised: (1) a well-defined depiction of iron irregularities in the substantia nigra; (2) a comparison between patients with Parkinson's disease (PD) and those with healthy controls (HC); (3) adherence to internationally recognized diagnostic criteria; (4) written in the English language. The human research committee at the Changshu Mingzhou Rehabilitation Hospital approved the study protocol after informed consent was given by all subjects. Based on the following search terms, papers were found by a computer literature search in July 2023: "parkinson disease" or "PD" or "Paralysis Agitans", "Magnetic Resonance Imaging" or "MRI", "substantia nigra" or "Nigra Substantia" or "Nigras Substantia" or "Substantia Nigras" or "nigra" or "SN", "iron" or "Ferric Compounds" or "Ferritins". 67 papers were duplicated and excluded. Of the remaining 413 abstracts, a further 388 were rejected due to irrelevant topics and improper types. A total of 25 full-text papers were retrieved, and only 16 of these papers met our inclusion criteria (Figure 1).

A review of the reference lists of these papers revealed no further studies for inclusion in our meta-analysis[11,15-29]. Two authors in our study independently reviewed all 16 articles and extracted and verified the data from each other. If two or more studies contained the same or overlap size of patients, only the largest one was chosen.

The manuscript was prepared and revised according to the PRISMA 2020 guidelines.

Statistical Analysis

Standardized mean difference (SMD) was used for continuous data, combining effect size (Hedge's g) to correct for small-scale bias. Heterogeneity was assessed using Cochran Q and I^2. If I^2 is <50%, suggesting greater homogeneity, a fixed-effects model was used for this homogenous analysis (I^2=25%) to calculate the pooled mean effect size. Sensitivity analysis suggests a significant difference in the overall effect (p<0.00001). The robustness of our findings was further enhanced by performing sensitivity analyses and subgroup analyses. An asymmetric funnel plot was used to assess publication bias. Analyses were performed with Review Manager (RevMan 5.3) for Windows.

Results

Study Characteristics

16 studies of SN iron deposition assessed by MRI in PD or HC satisfied our inclusion criteria (these studies included 435 PD and 355 HC). The pooled mean characteristics of included studies

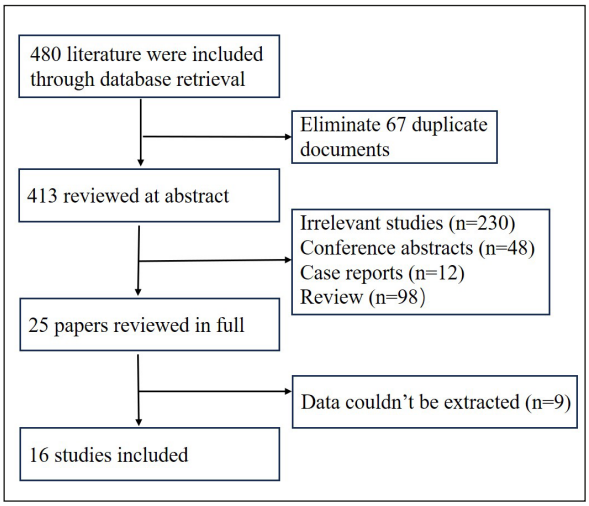

Figure 1. Flow diagram of article selection.

were as follows: age, range 50-66.5 years old; the number of males, range 5-42; the number of females, range 2-28; disease duration, range 1.65-9.04 years; Hoehn and Yahr (HY) stage, range 1.65-3; UPDRS-III motor score, range 11.38-34.6. The characteristics of the included studies are shown in Table I.

SN Iron Deposition

Iron deposition in SN was significantly greater in patients with PD than that in HC (SMD=0.72, 95% CI=0.57 to 0.87, $p<0.00001$, $Z=9.41$, 16 studies, n=790, Figure 2). Using I^2, a measure of the heterogeneity of the studies, showed that the studies in our meta-analysis were homogenous ($p=0.18$, $I^2=25\%$; Figure 2).

Further subgroup analyses were performed according to the following categories: "Image", "Disease duration", "H-Y stage", "UPDRS-III motor score". Detailed results of subgroup analysis were depicted in **Supplementary Figures 1-4**.

Each study was excluded sequentially from the sensitivity analysis. A significant overall effect ($p<0.00001$) was shown in Table II according to the sensitivity analysis.

No subgroup difference was detected in each category (Table III). In addition, R2* or SWI tended to have a larger effect than T2* (subgroup effect: "R2*": $Z=7.65$, $p<0.00001$, "SWI": $Z=5.24$ $p<0.00001$, "T2*": $Z=2.31$ $p=0.02$). The iron content of SN in patients with PD increased

Table I. Characteristics of studies included in this meta-analysis of SN iron content.

Study	Image	Group	Sample size	Male (female)	Age-yr	Disease Duration-yr	H-Y stage	UPDRS-III motor Score
Gorell et al[21] 1995	R2*	PD	13	11 (2)	65.2 ± 12.7	NA	NA	NA
		HC	9	5 (4)	60.0 ± 8.7			
Graham et al[19] 2000	R2*	PD	21	11 (10)	50.2 ± 9.5	11.1 ± 4.5	NA	NA
		HC	13	7 (6)	NA			
Wallis et al[11] 2008	R2*	PD	70	42 (28)	64.9	9.04	3	NA
		HC	10	5 (5)	57.2			
Zhang et al[18] 2010	SWI	PD	25	12 (13)	66.5 ± 8.1	3.4 ± 2.6	NA	19.0 ± 6.7
		HC	26	14 (12)	57.3 ± 11.6			
Lee et al[23] 2010	T2*	PD	20	12 (8)	62.2 ± 10.2	4.0 ± 2.3	1.65 ± 0.49	18.3 ± 6.1
		HC	20	12 (8)	62.3 ± 10.8			
Du et al[17] 2012	R2*	PD	40	23 (17)	60.7 ± 8.3	4.2 ± 4.7	1.75 ± 0.6	23.4 ± 15.2
		HC	29	12 (17)	59.6 ± 6.7			
Han et al[16] 2012	SWI	PD	15	7 (8)	57.4 ± 7.1	2.52 ± 1.6	2.2 ± 0.45	23.0 ± 5.6
		HC	20	12 (8)	55.9 ± 6.2			
Bunzeck et al[22] 2013	R2*	PD	20	11 (9)	66.3 ± 9.0	6.27 ± 4.4	NA	34.6 ± 17.4
		HC	20	10 (10)	66 ± 9.1			
Kim et al[15] 2014	SWI	PD	30	19 (11)	57.6 ± 6.8	1.65 ± 1.1	1.7 ± 0.47	24.5 ± 8.4
		HC	25	12 (13)	56.2 ± 6.5			
Barbosa et al[20] 2015	R2*	PD	20	12 (8)	66 ± 8	8.1 ± 4.2	2.25 ± 0.6	NA
		HC	30	9 (21)	64 ± 7			
Xuan et al[25] 2017	T2*	PD	35	17 (18)	50.0 ± 5.3	4.4 ± 3.4	2.1 ± 0.8	26.4 ± 17.6
		HC	24	11 (13)	51.8 ± 7.5			
Costa-Mallen et al[26] 2017	R2*	PD	24	11 (13)	63.6 ± 9.0	NA	2.1 ± 0.54	NA
		HC	27	14 (13)	64.0 ± 9.2			
Arribarat et al[27] 2019	R2*	PD	18	10 (8)	65.2 ± 6.6	6.83 ± 4.7	NA	11.38 ± 4.92
		HC	21	8 (13)	66 ± 4.91			
Cheng et al[29] 2020	R2*	PD	25	14 (11)	65.28 ± 8.32	4.56 ± 4	2.3 ± 0.66	NA
		HC	28	10 (18)	63.67 ± 9.58			
He et al[28] 2020	R2*	PD	39	17 (22)	63.4 ± 7.0	6.1 ± 4.5	1.7 ± 0.078	22.13 ± 12.64
		HC	33	14 (19)	63.8 ± 6.9			
Lee et al[24] 2021	R2*	PD	20	10 (10)	61 ± 4	5 ± 3	2.0 ± 0.4	18.5 ± 7.7
		HC	20	10 (10)	61 ± 3			

SN, substantia nigra; SWI, Susceptibility-Weighted Imaging; HY, Hoehn and Yahr stage; UPDRS, Unified Parkinson Disease Rating Scale; NA, not available; ROI, regions of interest; HC, healthy control; PD, Parkinson's disease; SMD, standardized mean difference.

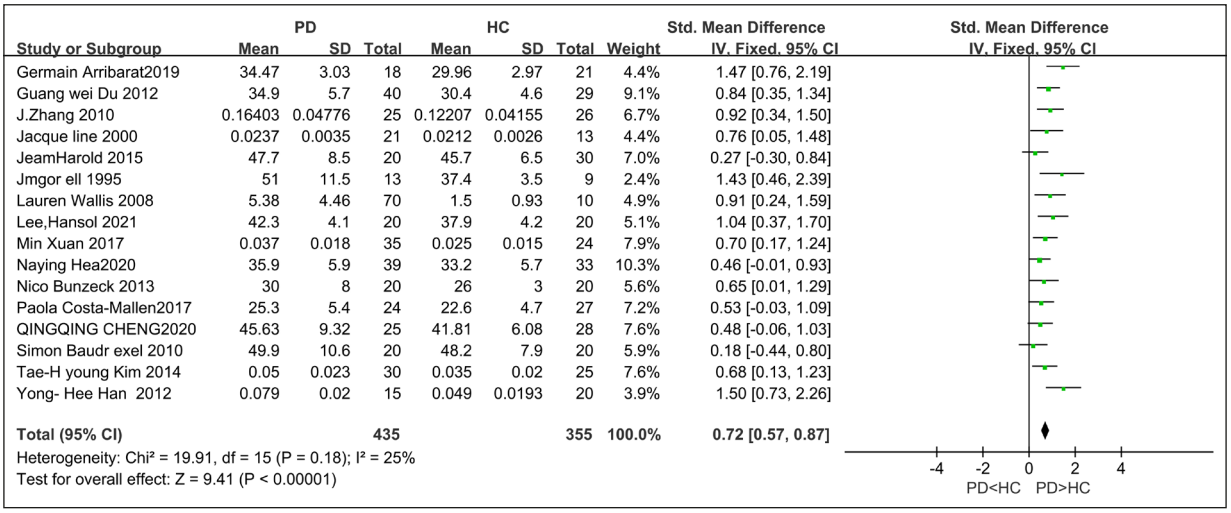

Figure 2. Forest plot of standardized mean difference (SMD) of substantia nigra (SN) iron deposition in Parkinson's disease (PD) and Health control (HC).

with a prolonged course of the disease, as our data showed (subgroup effect: Mean duration >4 years: Z=7.48, p<0.00001. Mean duration <=4 years, Z=4.84, p<0.00001). The deposition of iron within the SN was greater with increasing severity of PD, judged by UPDRS-III staging, compared to HC (subgroup effect: "UPDRS-III motor score Mean >20": Z=6.36, p<0.00001, Mean "UPDRS-III motor score <20": Z=5.28, p<0.0001) (Table III).

Publication Bias

When testing for publication bias, the funnel plot appeared to show asymmetry (Figure 3).

Discussion

Iron stored as ferritin exhibited high concentrations in the extrapyramidal system, such as SN, which contributes to the brain circuits responsible

Table II. Results of the sensitivity analysis for overall effect.

Excluded study	Group	Sample size (PD, HC)	SMD [95% CI]	Test for heterogeneity		Test for overall effect	
				I^2-%	p	Z	p
Arribarat et al[27] 2019	PD, HC	18, 21	0.69 [0.53, 0.84]	10%	0.34	8.76	p < 0.00001
Du et al[17] 2012	PD, HC	40, 29	0.71 [0.55, 0.87]	29%	0.14	8.82	p < 0.00001
Zhang et al[18] 2010	PD, HC	25, 26	0.71 [0.55, 0.86]	28%	0.15	8.9	p < 0.00001
Graham et al[19] 2000	PD, HC	21, 13	0.72 [0.57, 0.87]	30%	0.13	9.17	p < 0.00001
Barbosa et al[20] 2015	PD, HC	20, 30	0.76 [0.60, 0.91]	19%	0.24	9.5	p < 0.00001
Gorell et al[21] 1995	PD, HC	13, 9	0.71 [0.55, 0.86]	22%	0.21	9.07	p < 0.00001
Wallis et al[11] 2008	PD, HC	70, 10	0.71 [0.56, 0.87]	29%	0.14	9.05	p < 0.00001
Lee et al[24] 2021	PD, HC	20, 20	0.71 [0.55, 0.86]	26%	0.17	8.95	p < 0.00001
Xuan et al[25] 2017	PD, HC	35, 24	0.72 [0.57, 0.88]	30%	0.13	9.05	p < 0.00001
He et al[28] 2020	PD, HC	39, 33	0.75 [0.59, 0.91]	25%	0.18	9.28	p < 0.00001
Bunzeck et al[22] 2013	PD, HC	20, 20	0.73 [0.57, 0.88]	29%	0.13	9.2	p < 0.00001
Costa-Mallen et al[26] 2017	PD, HC	24, 27	0.74 [0.58, 0.89]	28%	0.15	9.25	p < 0.00001
Cheng et al[29] 2020	PD, HC	25, 28	0.74 [0.59, 0.90]	27%	0.16	9.29	p < 0.00001
Baudrexel et al[23] 2010	PD, HC	20, 20	0.76 [0.60, 0.91]	17%	0.27	9.56	p < 0.00001
Kim et al[15] 2014	PD, HC	30, 25	0.73 [0.57, 0.88]	30%	0.13	9.09	p < 0.00001
Han et al[16] 2012	PD, HC	15, 20	0.69 [0.54, 0.85]	12%	0.32	8.83	p < 0.00001

Table III. Results of subgroup analyses.

	Subgroup	Included study number	Sample size (PD, HC)	SMD [95% CI]	Test for heterogeneit within subgroup		Test for subgroup effect		Test for subgroup differences	
					I^2-%	p	Z	p	I^2-%	p
Image	R2*	11	310, 240	0.71 [0.53, 0.90]	20%	$p = 0.25$	7.65	$p < 0.00001$	31.4%	0.23
	SWI	3	70, 71	0.94 [0.59, 1.30]	31%	$p = 0.24$	5.24	$p < 0.00001$		
	T2*	2	55, 44	0.48 [0.07, 0.88]	36%	$p = 0.21$	2.31	$p = 0.02$		
Disease duration	Mean ≤ 4 years	4	90, 91	0.76 [0.45, 1.06]	59%	$p = 0.06$	4.84	$p < 0.00001$	0%	0.78
	Mean > 4 years	10	308, 228	0.71 [0.52, 0.89]	10%	$p = 0.35$	7.48	$p < 0.00001$		
H-Y stage	Mean ≤ 2.1	7	208, 178	0.63 [0.42, 0.83]	0%	$p = 0.55$	5. 95	$p < 0.00001$	0%	0.80
	Mean > 2.1	4	130, 88	0.68 [0.37, 0.99]	59%	$p = 0.06$	4.26	$p < 0.00001$		
UPDRS-III motor score	Mean < 20	4	83, 87	0.86 [0.54, 1.18]	61%	$p = 0.05$	5.28	$p < 0.00001$	0%	0.52
	Mean > 20	6	179, 151	0.73 [0.51, 0.96]	8%	$p = 0.37$	6.36	$p < 0.00001$		

CI, confidence interval; SWI, Susceptibility-Weighted Imaging; H-Y, Hoehn-Yahr; UPDRS, Unified Parkinson Disease Rating Scale; NA, not available; HC, Health control; PD, Parkinson's disease; SMD, standardized mean difference.

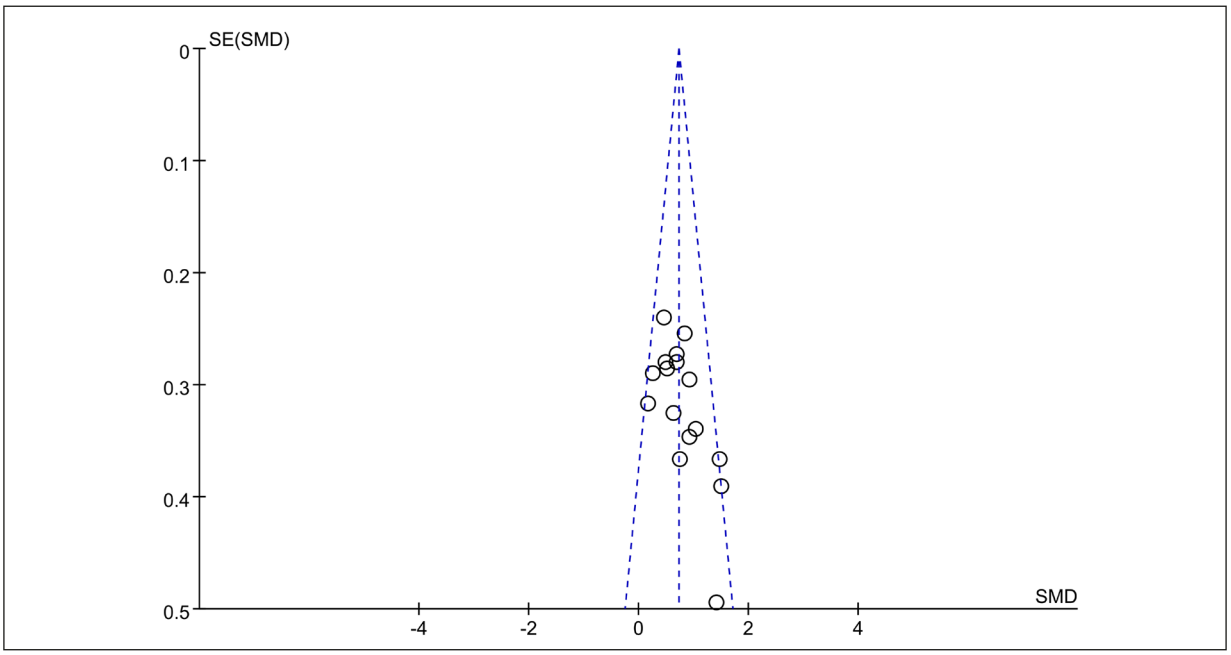

Figure 3. Funnel plot appeared to show asymmetry.

for involuntary movement[21]. In our meta-analysis, all 16 studies detected SN iron deposition in PD patients, consistent with the loss of dopaminergic neurons in SN, the neuropathological hallmark of PD. Labile iron deposition leads to neurotoxicity, triggering the death of dopaminergic cells and symptomatic motor defects in PD patients[8].

The SN iron accumulation assessed by MRI may provide a novel method to detect neuron loss *in vivo*. Our meta-analysis detected a large, pooled effect size for iron elevation in the SN of PD patients. In our meta-analysis, the I^2 of 25% reflects the homogeneity of the studies included, further suggesting that these results may be generalizable to a standard PD population. A robust sensitivity analysis in our study also supported this finding.

R2* and SWI are widely available and commonly used in MRI assessment, which could assess the SN iron accumulation to identify preclinical cases of PD[30]. Our subgroup analyses suggested that R2* and SWI might be a more sensitive method for imaging brain iron than other MRI analyses. In contrast with SWI, R2* has a lower sensitivity and specificity. SWI contributes enormously to the diagnosis of PD at an early stage. One recent study[31] using vector machine analysis (SVM) of SWI classified PD patients with an accuracy of more than 86%. By measuring the diffusion of water molecules, diffusion tensor imaging (DTI) determines the integrity of white matter tracts. Disruptions of microstructural tissue integrity in neurodegenerative diseases, such as PD, can lead to alterations in DTI. Multimodal imaging, combined with DTI and the assessment of SN iron deposition, may enhance the diagnostic sensitivity of PD in the future[32].

Previous studies[18,21,33,34] have demonstrated that iron concentrations of the SN were closely linked to the UPDRS-III motor score (r=0.361, p=0.022) in SWI (r=0.47, p=0.004) in T2*. We confirmed it, we found that the deposition of iron within the SN was greater with increasing severity of PD, judged by UPDRS-III staging. Besides, our subgroup analyses demonstrated that mean disease duration >4 years is related to more iron deposition in SN in patients with PD, compared with those mean disease duration <4 years. Therefore, SN iron content might be useful to monitor PD progression. Based on homogenous group analysis, MRI-based SN iron could also be a noninvasive imaging marker for PD.

It is important to note that there are a few limitations to the present study. Firstly, unpublished studies were not taken into account, and the research was restricted to papers only in English. Secondly, the number of studies that met our inclusion criteria was quite small. Lastly, there may be a possibility of publication bias for this meta-analysis, which cannot be ruled out.

Nevertheless, MRI assessment of SN iron appears to be a potentially valuable means for

identifying abnormal iron deposition in PD patients. This means that this imaging modality can play a vital role in early diagnosis and following progression of PD. Our findings based on homogeneous group-level analysis might indicate that MRI-based SN iron could be a potential way to differentiate individuals with PD from HC at an early stage of the disease. However, larger cohort studies are required to investigate SN iron elevation in PD more rigorously. Some studies[35,36] showed that quantitative susceptibility mapping and multimodal neuroimaging will be facilitated to get better reliability of the results. Because of the popularity and feasibility of MRI technology, we hope that the determination of iron content in SN by MRI could be a candidate for a biomarker for the diagnosis of PD in the future.

Conclusions

MRI assessment for the detection of SN iron deposition, including R2* or SWI, could be an early promising biomarker in patients with PD. Moreover, SN iron deposition evaluated by MRI may monitor the progression and severity of PD. However, since the sensibility of MRI may not be exactly clear, more sensitive methods are needed to explore.

Conflict of Interest
The authors declare that they have no conflict of interests.

Data Availability
Data supporting the findings of this study are available from the corresponding author upon reasonable request.

Authors' Contribution
All authors have already read and come to an agreement on this article. All authors have contributed significantly. Kai He guaranteed the integrity of the entire study. Gailing Liu was responsible for the study concepts and design. Haowen Zhang performed data and statistical analysis. Caobing Zha and Tingwei Fan completed the literature research. Shoutao Chen and Tiantian Shen prepared and edited the manuscript.

Funding
This work was supported by the Science and Technology Commission Foundation of college project (shdlyy202201).

Informed Consent
Not applicable.

Ethics Approval
Not applicable.

ORCID ID
K. He: 0009-0009-3776-9693

References

1) Kalia LV. Parkinson's disease. Lancet 2015; 386: 896-912.
2) DW D. Parkinson's disease and parkinsonism: neuropathology. Cold Spring Harb Perspect Med 2012; 2: a009258.
3) Rizzo G, Copetti M, Arcuti S, Martino D, Fontana A, Logroscino G. Accuracy of clinical diagnosis of Parkinson disease: A systematic review and meta-analysis. Neurology 2016; 86: 566-576.
4) Shao Y, Le W. Recent advances and perspectives of metabolomics-based investigations in Parkinson's disease. Mol Neurodegener 2019; 14: 3.
5) Li T, Le W. Biomarkers for Parkinson's Disease: How Good Are They? Neurosci Bull 2020; 36: 183-194.
6) Lhermitte J, Kraus WM, McAlpine D. On the occurrence of abnormal deposits of iron in the brain in Parkinsonism with special reference to its localization. J Neurol Psychopathol 1924; 5: 195-208.
7) Sofic E, Riederer P, Heinsen H, Beckmann H, Reynolds GP, Hebenstreit G, Youdim MB. Increased iron (III) and total iron content in post-mortem substantia nigra of Parkinsonian brain. J Neural Transm 1988; 74: 199-205.
8) Wypijewska A, Galazka-Friedman J, Bauminger ER, Wszolek ZK, Schweitzer KJ, Dickson DW, Jaklewicz A, Elbaum D, Friedman A. Iron and reactive oxygen species activity in parkinsonian substantia nigra. Parkinsonism Relat Disord 2010; 16: 329-333.
9) Xu X, Wang Q, Zhang M. Age, gender, and hemispheric differences in iron deposition in the human brain: an in vivo MRI study. Neuroimage 2008; 40: 35-42.
10) Ye FQ, Allen PS, Martin WR. Basal ganglia iron content in Parkinson's disease measured with magnetic resonance. Mov Disord 1996; 11: 243-249.
11) Wallis LI, Paley MN, Graham JM, Grunewald RA, Wignall EL, Joy HM, Griffiths PD. MRI assessment of basal ganglia iron deposition in Parkinson's disease. J Magn Reson Imaging 2008; 28: 1061-1067.
12) Haacke EM, Cheng NY, House MJ, Liu Q, Neelavalli J, Ogg RJ, Khan A, Ayaz M, Kirsch W, Obenaus A. Imaging iron stores in the brain using magnetic resonance imaging. Magn Reson Imaging 2005; 23: 1-25.
13) Du G, Lewis MM, Styner M, Shaffer ML, Sen S, Yang QX, Huang X. Combined R2* and diffusion tensor imaging changes in the substantia nigra in

Parkinson's disease. Mov Disord 2011; 26: 1627-1632.

14) Gelb DJ, Oliver E, Gilman S. Diagnostic criteria for Parkinson disease. Arch Neurol 1999; 56: 33-39.

15) Kim TH, Lee JH. Serum uric acid and nigral iron deposition in Parkinson's disease: a pilot study. PLoS One 2014; 9: e112512.

16) Han YH, Lee JH, Kang BM, Mun CW, Baik SK, Shin YI, Park KH. Topographical differences of brain iron deposition between progressive supranuclear palsy and parkinsonian variant multiple system atrophy. J Neurol Sci 2013; 325: 29-35.

17) Du G, Lewis MM, Shaffer ML, Chen H, Yang QX, Mailman RB, Huang X. Serum cholesterol and nigrostriatal R2* values in Parkinson's disease. PLoS One 2012; 7: e35397.

18) Zhang J, Zhang Y, Wang J, Cai P, Luo C, Qian Z, Dai Y, Feng H. Characterizing iron deposition in Parkinson's disease using susceptibility-weighted imaging: an in vivo MR study. Brain Res 2010; 1330: 124-130.

19) Graham JM, Paley MN, Grünewald RA, Hoggard N, Griffiths PD. Brain iron deposition in Parkinson's disease imaged using the PRIME magnetic resonance sequence. Brain 2000; 123 Pt 12: 2423-2431.

20) Barbosa JH, Santos AC, Tumas V, Liu M, Zheng W, Haacke EM, Salmon CE. Quantifying brain iron deposition in patients with Parkinson's disease using quantitative susceptibility mapping, R2 and R2. Magn Reson Imaging 2015; 33: 559-565.

21) Gorell JM, Ordidge RJ, Brown GG, Deniau JC, Buderer NM, Helpern JA. Increased iron-related MRI contrast in the substantia nigra in Parkinson's disease. Neurology 1995; 45: 1138-1143.

22) Bunzeck N, Singh-Curry V, Eckart C, Weiskopf N, Perry RJ, Bain PG, Duzel E, Husain M. Motor phenotype and magnetic resonance measures of basal ganglia iron levels in Parkinson's disease. Parkinsonism Relat Disord 2013; 19: 1136-1142.

23) Baudrexel S, Nurnberger L, Rub U, Seifried C, Klein JC, Deller T, Steinmetz H, Deichmann R, Hilker R. Quantitative mapping of T1 and T2* discloses nigral and brainstem pathology in early Parkinson's disease. Neuroimage 2010; 51: 512-520.

24) Lee H, Cho H, Lee MJ, Kim TH, Roh J, Lee JH. Differential Effect of Iron and Myelin on Susceptibility MRI in the Substantia Nigra. Radiology 2021; 301: 682-691.

25) Xuan M, Guan X, Gu Q, Shen Z, Yu X, Qiu T, Luo X, Song R, Jiaerken Y, Xu X, Huang P, Luo W, Zhang M. Different iron deposition patterns in early- and middle-late-onset Parkinson's disease. Parkinsonism Relat Disord 2017; 44: 23-27.

26) Costa-Mallen P, Gatenby C, Friend S, Maravilla KR, Hu SC, Cain KC, Agarwal P, Anzai Y. Brain iron concentrations in regions of interest and relation with serum iron levels in Parkinson disease. J Neurol Sci 2017; 378: 38-44.

27) Arribarat G, Pasternak O, De Barros A, Galitzky M, Rascol O, Péran P. Substantia nigra locations of iron-content, free-water and mean diffusivity abnormalities in moderate stage Parkinson's disease. Parkinsonism Relat Disord 2019; 65: 146-152.

28) He N, Langley J, Huddleston DE, Chen S, Huang P, Ling H, Yan F, Hu X. Increased iron-deposition in lateral-ventral substantia nigra pars compacta: A promising neuroimaging marker for Parkinson's disease. Neuroimage Clin 2020; 28: 102391.

29) Cheng Q, Huang J, Liang J, Ma M, Zhao Q, Lei X, Shi C, Luo L. Evaluation of abnormal iron distribution in specific regions in the brains of patients with Parkinson's disease using quantitative susceptibility mapping and R2* mapping. Exp Ther Med 2020; 19: 3778-3786.

30) Stoessl AJ, Martin WW, McKeown MJ, Sossi V. Advances in imaging in Parkinson's disease. Lancet Neurol 2011; 10: 987-1001.

31) Haller S, Badoud S, Nguyen D, Barnaure I, Montandon ML, Lovblad KO, Burkhard PR. Differentiation between Parkinson disease and other forms of Parkinsonism using support vector machine analysis of susceptibility-weighted imaging (SWI): initial results. Eur Radiol 2013; 23: 12-19.

32) Aquino D, Contarino V, Albanese A, Minati L, Farina L, Grisoli M, Romita L, Elia AE, Bruzzone MG, Chiapparini L. Substantia nigra in Parkinson's disease: a multimodal MRI comparison between early and advanced stages of the disease. Neurol Sci 2014; 35: 753-758.

33) Péran P, Cherubini A, Assogna F, Piras F, Quattrocchi C, Peppe A, Celsis P, Rascol O, Démonet JF, Stefani A, Pierantozzi M, Pontieri FE, Caltagirone C, Spalletta G, Sabatini U. Magnetic resonance imaging markers of Parkinson's disease nigrostriatal signature. Brain 2010; 133: 3423-3433.

34) Wang C, Fan G, Xu K, Wang S. Quantitative assessment of iron deposition in the midbrain using 3D-enhanced T2 star weighted angiography (ESWAN): a preliminary cross-sectional study of 20 Parkinson's disease patients. Magn Reson Imaging 2013; 31: 1068-1073.

35) Chen Q, Chen Y, Zhang Y, Wang F, Yu H, Zhang C, Jiang Z, Luo W. Iron deposition in Parkinson's disease by quantitative susceptibility mapping. BMC Neurosci 2019; 20: 23.

36) Depierreux F, Parmentier E, Mackels L, Baquero K, Degueldre C, Balteau E, Salmon E, Phillips C, Bahri MA, Maquet P, Garraux G. Parkinson's disease multimodal imaging: F-DOPA PET, neuromelanin-sensitive and quantitative iron-sensitive MRI. NPJ Parkinsons Dis 2021; 7: 57.